

Mixed Ion and Electron Conducting Ceramics for Gas Sensors

S. Mulmi, R. Kannan, and V. Thangadurai*

Department of Chemistry, University of Calgary, Calgary, Alberta, T2N 1N4, Canada.

A conventional solid-state synthetic route was used to prepare a mixed conducting double perovskite-type $\text{Ba}_2\text{Ca}_{0.66}\text{Nb}_{0.68}\text{Fe}_{0.66}\text{O}_{6-\delta}$ (BCNF66). FTIR study was performed to confirm the chemical stability under 1% CO_2 , whereas the cross-sectional SEM image was employed to investigate the morphology of the sensor. A comparative study on BCNF66 with and without CO_2 in dry synthetic air along with O_2 effect was carried out. The significant effect of O_2 was observed when CO_2 was passed through the sensor in N_2 . The O_2 in dry synthetic air was found to stabilize the CO_2 sensor response (current). Furthermore, the addition of ppm level of CO_2 in dry synthetic air increased the response.

Introduction

Sensors based on solid-state electrolytes are favorably utilized for the detection of various gaseous species because of their high selectivity characteristics. So far, only few solid-state electrolyte based sensors have been practically employed. For example, stabilized zirconia has been successfully used in the fields of steel industries, combustion control and automobiles as a reliable O_2 sensor. In case of CO_2 , measuring its concentration in atmosphere and several industrial processes is highly desirable because of its direct impact on climate change. Carbon capture and storage (CCS), a major solution to cope with these global warming issues, also requires online gas detecting devices that could sustain in presence of various gases at high temperatures (1-3). Furthermore, the real-time online monitoring of the gaseous composition in the industrial processes has become essential for reducing the emissions and improving its efficiency (4). Solid-state electrochemical sensors are well suited in harsh and aggressive conditions such as high temperatures and high pressures (5, 6). Fast alkali ion-conducting materials and semiconducting materials have been developed to measure the CO_2 (1, 7-11). However, several critical issues such as low chemical stability at high temperature, poor performance in humid conditions and low selectivity due to influences by other gases have remained (12, 13).

Recently, we reported double perovskite-based mixed ion and electron conductor (MIEC), $\text{Ba}_2\text{Ca}_{0.66}\text{Nb}_{1.34-x}\text{Fe}_x\text{O}_{6-\delta}$ (BCNF), to overcome the existing problems in solid-state electrochemical CO_2 sensors (14). The mixed conducting Fe-doped BCNF exhibited good CO_2 sensing performance, for example, $\text{Ba}_2\text{Ca}_{0.66}\text{Nb}_{0.68}\text{Fe}_{0.66}\text{O}_{6-\delta}$ (BCNF66) showed high sensitivity and fast response with good selectivity in presence of SO_2 (15). For the preparation of gas mixture, however, CO_2 was diluted with dry synthetic air at different ratios. In general, researchers have carried out numerous experiments in presence of O_2 because of its significant role in chemical reactions during sensing measurements (2, 16). In our earlier work, the exact role of O_2 in CO_2 sensors was not studied. Therefore, in this study, we have tested role of O_2 on CO_2 sensing properties of BCNF66.

Experimental

Sample Preparation and Characterization

BCNF66 was prepared by a conventional ceramic method using stoichiometric amounts of $\text{Ba}(\text{NO}_3)_2$ (99+%, Alfa Aesar), CaCO_3 , (99% Fisher Scientific Company), Nb_2O_5 (99.5%, Alfa Aesar) and Fe_2O_3 (99+%, Alfa Aesar). The reactant powders were mixed and ball-milled (Pulverisette Fritsch, Germany) with 2-propanol for 6 h at 200 rpm using zirconia balls with reversed rotation every 30 mins. The mixture was dried in an oven (~80 °C) and ground into fine powder using agate mortar and pestle. The powder was then calcined at 1000 °C in air for 12 h and mixed again for 6 h using ball-mill. Thus, the obtained fine powder was isotactically pressed into pellets (10 mm in diameter, 1 mm in thickness) followed by sintering at 1350 °C for 24 h. The sintered pellets were used for the sensor studies. Powder X-ray diffraction (PXRD) (Bruker D8 Advance, CuK_α ; 40 kV; 40 mA) was used to confirm the phase formation (14).

A Varian 7000 FTIR spectrometer was employed for the chemical stability test under the CO_2 atmosphere. 1% CO_2 balanced in dry synthetic air was purged into the powdered sample kept in an alumina boat, which was later inserted inside a gas-tight quartz tube followed by heating the furnace at 700 °C for 72 h. Scanning electron microscopy (SEM) (Philips XL30 SEM) was used to study the microstructure of the BCNF66 pellet.

Sensing Cell Fabrication

For the fabrication of the sensing cell, a porous Au-layer was coated on both sides of BCNF66 pellet as current-collectors by a paint-brushing method and dried at 600 °C for an hour to remove the organic binders present in Au-paste. The Au-coated BCNF66 pellet was kept between alumina pellets with Au wire connected on each side of the BCNF66 pellet with the help of spring-loaded contact cell. The cell was heated up to 700 °C and left for at least 6 h before measuring the sensing properties.

DC measurement (Solartron, model SI 1287) was carried out by applying a constant dc voltage of 0.1 V on BCNF66 pellet at different ppm level of CO_2 gas. The gases used for the sensing measurements were N_2 , O_2 , 3000 ppm CO_2 in dry synthetic air (21% O_2 in N_2) and pure CO_2 (99.99%) (Praxair Inc., Canada). The amount of gas inside the cell was handled by using the computer-controlled mass flow controllers (MCS-100 SCCM-D/5M, 5IN). The total flow rate of the gas was maintained at 100 sccm. Table I lists the investigated gas compositions. The fabricated sensor was kept at the middle of tubular furnace inside an air-tight quartz tube. The measurements were typically carried out at 700 °C.

Results and Discussion

We have shown that BCNF66 is chemically stable under CO_2 environment by employing an *in-situ* high-temperature powder X-ray diffraction (HT-PXRD). Cubic single-phase double perovskite-type structure with $Fm-3m$ space group was further confirmed using high-resolution transmission electron microscopy (HRTEM) coupled with selected area electron diffraction (SAED) (14). FTIR measurement on 1% CO_2 treated BCNF66 was

carried out to understand the carbonate formation in BCNF66. No absorption bands were seen at 1750 and 2452 cm^{-1} for BCNF66 after CO_2 treatment at 700 $^\circ\text{C}$ for 72 h as shown in Figure 1a. In general, 1750 cm^{-1} and 2452 cm^{-1} bands, as shown for commercial BaCO_3 in Figure 1a, are specifically assigned to the $\nu_1 + \nu_4$ combination mode of carbonate anion, and hydroxyl mode of hydrogen carbonate that usually forms on the surface when exposed to air, respectively (17). The results from FTIR suggest that the BCNF66 is highly stable in 1 % CO_2 at the investigated condition.

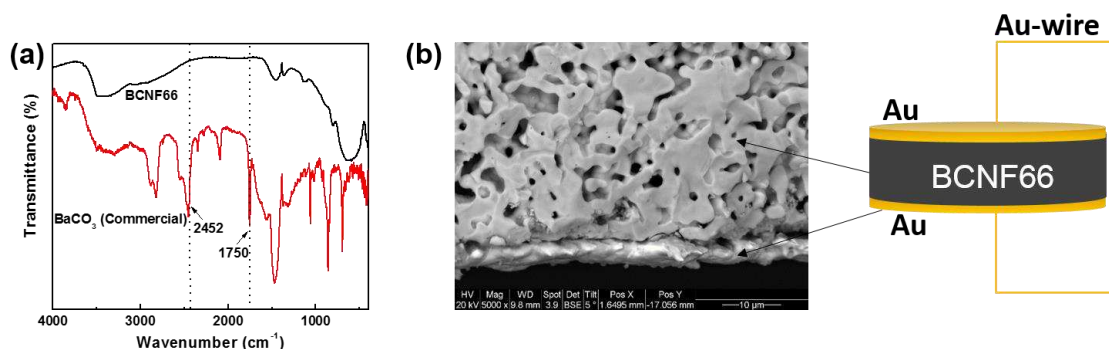


Figure 1. (a) FTIR spectra of BCNF66 after exposing to 1% CO_2 balanced in dry synthetic air at 700 $^\circ\text{C}$ for 72 h and FT-IR spectra of commercial BaCO_3 . (b) Cross-sectional SEM image showing Au-layer pasted on BCNF66 surface with a cartoon representation of the sensing cell.

A cross-sectional SEM image of BCNF66 with Au current collector layer is shown in Figure 1b. The SEM image showed the existing pores inside BCNF66, where the closed pore size varied from 1-6 μm in average. In addition, the formation of grains can also be observed inside the pores with its size in the range of 1-3 μm .

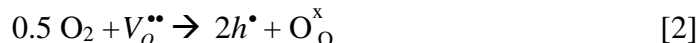
Table I. Gas Composition Used for Sensing Measurements

N ₂ (sccm)	3000 ppm CO ₂ in Dry Synthetic Air (sccm)		
	N ₂	O ₂	CO ₂ (in ppm)
96.67	2.62	0.70	100
83.33	13.13	3.49	500
66.67	26.25	6.98	1000
50	39.38	10.47	1500

Table I shows the gas mixture employed in the sensor study. According to Table I, O₂ was varied from 0.70 % (at 100 ppm CO₂ level) to 10.47 % (at 1500 ppm CO₂ level). Therefore, two major sensing tests were carried out to separate the CO₂ effect out from O₂ effect in BCNF66. Test 1: Mixing N₂ and O₂ without CO₂ (gas mixture using first three columns in Table I) and Test 2: Mixing N₂, O₂ with CO₂ in ppm level. Test 2 with CO₂ showed the higher current densities comparing to Test 1 (without CO₂) keeping the flow rate constant (100 sccm) (18). This phenomenon could be due to the higher amount of O₂ present when CO₂ is purged with dry synthetic air followed by conversion of O₂ to O²⁻. The dissociation of CO₂ into CO and O₂ can be expressed as:



It seems that Fe in BCNF66 is involved in catalytic reaction, and hence, reducing the electrical impedance as it acts as *p*-type semiconducting MIEC described by following expression (Eq. 2),



where $\text{O}_{\text{O}}^{\times}$, h^{\bullet} , and $V_{\text{O}}^{\bullet\bullet}$ correspond to the lattice O_2 , holes and oxide ion vacancies, respectively. Further details on sensing mechanism are discussed in our previous studies (15, 19). In Figure 2a, the response current densities for Test 1 and Test 2 are shown as open and closed symbols, respectively. The observed result in Figure 2a displays the CO_2 effect. Both sensing tests i.e., with and without CO_2 exhibit linear response as a function of logarithmic rise in O_2 content. Further, the difference in current densities between Tests 1 and 2 for each mixing ratio also increased with the increase in ppm level of CO_2 in dry synthetic air. Therefore, the difference of current densities (Δi_{CO_2}) in Test1 (i_{Test_1}) and Test 2 (i_{Test_2}) is given by:

$$\Delta i_{\text{CO}_2} = i_{\text{Test}_2} - i_{\text{Test}_1} \quad [3]$$

Interestingly, we found a linear relation between Δi_{CO_2} and $\log \text{CO}_2$.

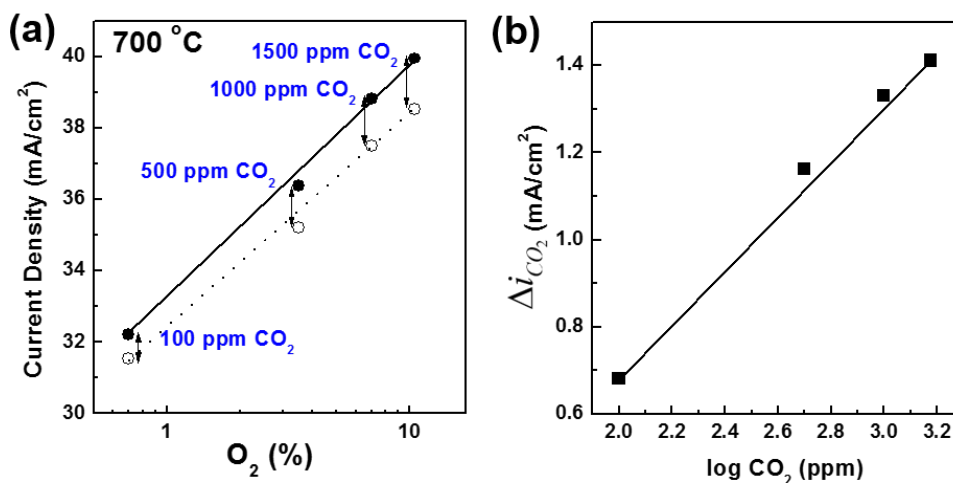


Figure 2. Current density as a function of O_2 content in dry synthetic air (open symbols) and O_2 content in presence of ppm level of CO_2 (closed symbols). (b) Response current density due to ppm level of CO_2 at each level (gas composition given in Table I). The line passing through the data points guide to the eye.

For further understanding of the role of O_2 Test 3 and Test 4 were performed in the similar environment (700 °C, 0.1V), where pure N_2 was used as our base gas for dilution. Test 3: Mixing pure N_2 and 1500 ppm CO_2 balanced in N_2 without O_2 and Test 4: Mixing pure N_2 and pure CO_2 without O_2 (1% CO_2 in N_2). For Test 3, significant changes in the current densities were not observed. The signal to noise ratio was very low and we could not see the difference under the investigated condition. However, in case of Test 4,

significant change was observed after purging 1% CO₂ in N₂ as shown in Figure 3. In addition, a steady-state current was not obtained in Test 4. The response quickly dropped into its original current density value. Comparing the Test 4 result with Test 1 and 2, where O₂ is mixed, it can be concluded that O₂ seems to stabilize the response current. However, further research is required to understand the BCNF's CO₂ sensing behavior in presence as well as absence of O₂.

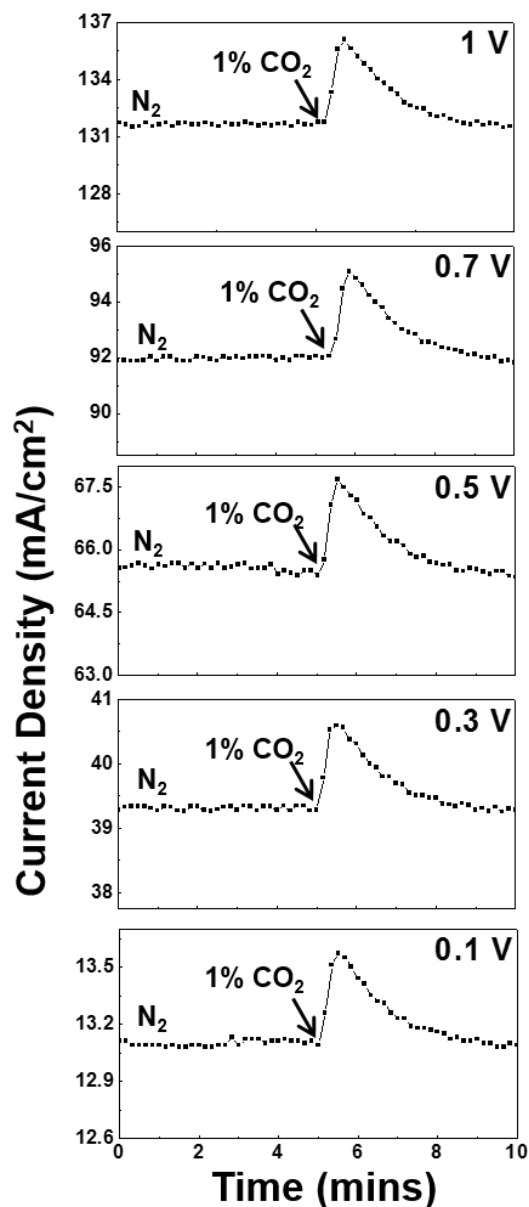


Figure 3. Current density as a function of time at various applied voltage (0.1-1 V).

Conclusion

Double perovskite-type Ba₂Ca_{0.66}Nb_{0.68}Fe_{0.66}O_{6-δ} (BCNF66) has been prepared by conventional solid-state method at elevated temperature in air. FTIR measurement was performed to confirm BCNF66's stability under CO₂. Further, a cross-sectional SEM image was taken to see the morphology after the sensor fabrication. A comparative study

on the effect of O₂ and CO₂ was carried out on BCNF66 by purging dry synthetic air with and without CO₂ (in ppm level), where the addition of CO₂ in dry synthetic air tends to increase the response current. The presence of O₂ in CO₂ shows the steady state current, while CO₂ only in N₂ could not achieve the equilibrium current. Future work on sensing measurements with different CO₂ concentrations and fixed O₂ are required to further understand BCNF66's sensing behavior with and without O₂.

Acknowledgments

The Institute for Sustainable Energy, Environment and Economy (ISEEE) of the University of Calgary, Natural Resources Canada and Carbon Management Canada (CMC) supported this work. The authors would like to express their sincere appreciation to Prof. Viola Birss (University of Calgary) and Prof. Abdelhamid Sayari (University of Ottawa) for their enthusiastic participation in discussions and helpful advice during our research. One of us, Suresh Mulmi, is thankful to Alberta Innovates Technology Futures (AITF) for graduate scholarship.

References

1. J. W. Fergus, *Sens. Actuators, B*, **134**, 1034 (2008).
2. H. H. Mobius, *J. Solid State Electrochem.*, **8**, 94 (2004).
3. C. V. Leeuwen, A. Hensen and H. A. J. Meijer, *Int. J. Greenhouse Gas Control*, **19**, 420 (2013)
4. N. Yamazoe, *Sens. Actuators, B*, **108**, 2 (2005).
5. W. Weppner, *Sens. Actuators*, **12**, 107 (1987).
6. C. O. Park, J. W. Fergus, N. Miura, J. Park and A. Choi, *Ionics*, **15**, 261 (2009).
7. N. Yamazoe and N. Miura, *Sens. Actuators, B*, **20**, 95 (1994).
8. M. Morio, T. Hyodo, Y. Shimizu and M. Egashira, *Sens. Actuators, B*, **139**, 563 (2009).
9. E. Steudel, P. Birke and W. Weppner, *Electrochim. Acta*, **42**, 3147 (1997).
10. Y. Zhu, V. Thangadurai and W. Weppner, *Sens. Actuators, B*, **176**, 284 (2013).
11. S. M. Kanan, O. M. El-Kadri, I. A. A. Yousef and M. C. Kanan, *Sensors*, **9**, 8158 (2009).
12. K. Obata, K. Shimanoe, N. Miura and N. Yamazoe, *Sens. Actuators, B*, **93**, 243 (2003).
13. E. D. Bartolomeo and E. Traversa, *J. Sol-Gel Sci. Technol.* **19**, 181 (2000).
14. S. Mulmi, A. Hassan, P. P. Almas and V. Thangadurai, *Sens. Actuators, B*, **178**, 598 (2013).
15. S. Mulmi, R. Kannan and V. Thangadurai, *Solid State Ionics*, in press, (2013).
doi: <http://dx.doi.org/10.1016/j.ssi.2013.09.050>
16. P. Pasierb and M. Rekas, *J. Solid State Electrochem*, **13**, 3 (2009).
17. E. Roedel, A. Urakawa, S. Kureti and A. Baiker, *Phys. Chem. Chem. Phys.*, **10**, 6190 (2008).
18. S. Mulmi and V. Thangadurai, *J. Electrochem. Soc.*, **160**, B95 (2013).
19. R. Kannan, S. Mulmi and V. Thangadurai, *J. Mater. Chem. A*, **1**, 6874 (2013).